Development of a $^{171}Yb^{+}$ Microwave Frequency Standard at the National Measurement Institute, Australia

R. B. Warrington, P. T. H. Fisk, M. J. Wouters, M. A. Lawn, J. J. Longdell and S. J. Park
National Measurement Institute
Lindfield, Australia
Bruce.Warrington@measurement.gov.au

***Abstract*—Microwave frequency standards based on the 12.6 GHz ground state hyperfine transition in $^{171}Yb^{+}$ have been under development at the National Measurement Institute, Australia, for many years. Using a laser-cooled ion cloud, the transition frequency was measured in 2001 to an accuracy of 8 parts in 10^{14}, limited by the homogeneity of the magnetic field due to the stainless-steel vacuum chamber. We have designed and commissioned a new chamber in the novel alloy CrCu, which is non-magnetic and has good vacuum properties. The design incorporates large viewports and high-quality quartz windows for optical access. Uncertainties associated with field inhomogeneity in the new vacuum system are now below 1 part in 10^{15}, a significant reduction which permits operation in the 10^{-15} accuracy range. We have also demonstrated the use of photoionization to load the trap in a preliminary experiment, including isotope-selective loading.**

I. Introduction

Microwave frequency standards based on the 12.6 GHz ground-state hyperfine ('clock') transition in trapped $^{171}Yb^{+}$ ions have demonstrated a stability characterised by a fractional Allan deviation $\sigma_y(\tau) = 5\times10^{-14}\ \tau^{-1/2}$ and a frequency uncertainty of ±1.1 parts in 10^{13} when operated with a He buffer gas for ion cooling [1,2]. The greatest contribution to the frequency uncertainty is the second-order Doppler shift due to the ion thermal motion, which can be reduced by eliminating the buffer gas and laser cooling the ions to sub-Kelvin temperatures [3–5].

We have previously reported microwave spectroscopy of laser-cooled $^{171}Yb^{+}$ [4], completed an extensive series of measurements of the ion temperature to quantify the remaining second-order Doppler shifts [5] and made a preliminary measurement of the clock transition frequency using a laser-cooled ion cloud [3]. The limiting uncertainty for this measurement was due to residual magnetic field inhomogeneity associated with the stainless steel ultra-high vacuum (UHV) chamber. Recent work has concentrated on reducing magnetic uncertainties by commissioning a new UHV chamber in novel non-magnetic materials, and on a simple test of photoionization to load the trap.

II. The Microwave Frequency Standard

A. Experimental Apparatus

The trapped-ion frequency standards at the National Measurement Institute, Australia (NMIA) have been described previously [1]. A linear Paul trap (Fig. 1) operates inside a UHV chamber at a base pressure below 1×10^{-10} Torr. The chamber is surrounded by four layers of magnetic shielding, and the ambient magnetic field inside the shields is controlled using three-axis Helmholtz coils plus additional coils to compensate for residual gradients.

The Yb^{+} resonance transition near 369 nm (Fig. 2) is used for both laser cooling, and to prepare and probe the populations of the ground state levels; this light is generated by a Coherent frequency-doubled titanium-doped sapphire laser. A small fraction of the ions decay to the metastable $^2D_{3/2}$ level; the transition at 935 nm returns these ions to the cooling cycle, using light generated by an external-cavity semiconductor laser diode. Finally, the transition between the ground state hyperfine levels is the reference frequency for the standard. Microwave radiation near 12 642 812 120 Hz for spectroscopy of this transition is synthesized from a sapphire-loaded superconducting dielectric resonator oscillator [6]. This radiation is also applied during cooling, in order to drain population accumulating in the lower hyperfine level.

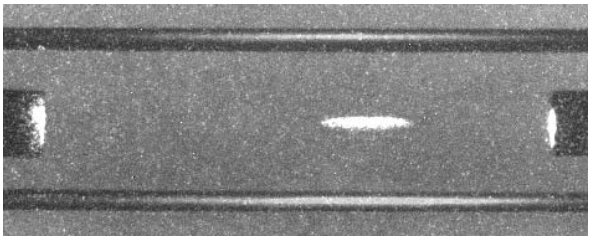

Figure 1. A laser-cooled $^{171}Yb^{+}$ ion cloud, approximately 10 mm long with a radius of 1.5 mm. RF electrodes of the linear Paul trap are visible top and bottom (diameter 2.3 mm, separation 20 mm) and DC electrodes left and right (separation 60 mm).

0-7803-9052-0/05/$20.00 © 2005 IEEE.

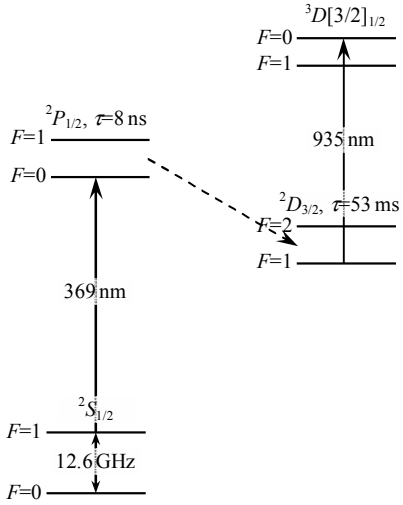

Figure 2. Partial energy level diagram of the $^{171}Yb^+$ ion.

Following loading, the RF and DC potentials of the linear trap are reduced for laser cooling. The fluorescence decreases sharply as the cloud approaches its coldest temperature, but it is likely that this 'phase transition' is to a liquid-like rather than a crystalline state [7]: we calculate a Coulomb coupling parameter (the ratio of electrostatic potential energy to thermal energy k_BT) of $\eta \sim 0.5$ at T=0.4 K, well below the transition value observed for large ion crystals [8].

B. Measurement of the Transition Frequency

Spectroscopy of the $M_F = 0 \rightarrow 0$ 'clock' hyperfine component of the 12.6 GHz transition uses Ramsey's method, with two $\pi/2$ pulses of length t=400 ms separated by t_R=10 s between pulse centres. The 369 nm light is blocked during the interrogation sequence to prevent light shifts, then reapplied to record the ion fluorescence as a measure of the microwave absorption. The ion cloud is subsequently re-cooled for 2 s, with the microwave field switched off for the last part of the cooling to optically pump the ions into the lower hyperfine state for the next interrogation. The microwave frequency is adjusted to match the ion transition by recording fluorescence at the half-height points of the central fringe. The ambient magnetic field is determined from the Larmor frequency ν, obtained by similarly tracking the $M_F = 0 \rightarrow \pm 1$ Zeeman component using Ramsey pulses with t=1 ms and t_R=2 ms. A measurement cycle consists of a frequency measurement (two count periods) for both the clock and Zeeman components, with a cycle time of approximately 40 s.

The absolute frequency calibration of the applied microwave field is conducted in two stages. A 2.88 GHz frequency signal derived from the sapphire resonator is directly compared to a similar signal from a hydrogen maser, which must then be separately compared to the SI second. Since the only local cesium references are commercial beam standards with insufficient frequency accuracy, the calibration must be made by common-view GPS frequency transfer. The corresponding uncertainty (5 parts in 10^{14}) was sufficient for the preliminary measurement [3], but more precise methods will be required once the systematic uncertainty in the frequency measurements reaches projected levels.

C. Systematic shifts

A full evaluation of systematic shifts for the microwave frequency standard is beyond the scope of this paper. Here we discuss the two largest shifts, the second-order Doppler and second-order Zeeman shifts, and refer to [3] for additional detail.

Second-order Doppler shifts are associated with both the driven (micromotion) and free (secular) components of the ion motion in the usual pseudopotential approximation. The micromotion component may be readily calculated [3], with a mean shift for the ion cloud proportional to the square of the cloud radius r. We obtain a shift of approximately $(6\pm2)\times10^{-15}$ for an ellipsoid with r=1 mm (typical), where the uncertainty is conservative. This is of the same order as, or smaller than, the collisional shift in a cesium fountain. The shift associated with thermal motion must be characterized separately by measuring the kinetic energy of secular motion, or equivalently the effective secular temperature obtained from the lineshape of the resonance transition [5]. Although this temperature rises during the microwave interrogation since the cooling light must be blocked to prevent light shifts, the corresponding second-order Doppler shift remains below 1×10^{-15} for Ramsey intervals t_R up to 10 s and beyond.

The second-order Zeeman shift is obtained from the Larmor frequency ν using standard expressions. The uncertainty Δ in this correction scales as the product $\nu\cdot\delta\nu$, where the uncertainty $\delta\nu$ is conservatively taken to be the FWHM of the Zeeman component pending a detailed investigation of the lineshape. For the preliminary measurement [3], ν~17 kHz, $\delta\nu$~75 Hz and $\Delta=3\times10^{-14}$. Using compensation coils to minimise magnetic field gradients (and consequently $\delta\nu$), the uncertainty Δ could be temporarily improved by an order of magnitude to $\Delta=2\times10^{-15}$ (Fig. 3). However, ν and particularly $\delta\nu$ were not sufficiently stable to maintain this level of uncertainty for sustained operation.

We believe that unavoidable stray fields associated with the UHV chamber itself set a fundamental limit on the homogeneity of the magnetic field which can be readily achieved in practice. The chamber for the preliminary measurement was constructed of stainless steel (the low-magnetic alloy 316 LN), and attempts to degauss this chamber did not yield significant improvement in the magnetic environment. It was therefore decided to construct a new UHV chamber entirely from non-magnetic materials, to eliminate stray magnetic fields as far as possible and improve the homogeneity of the ambient magnetic field across the ion cloud.

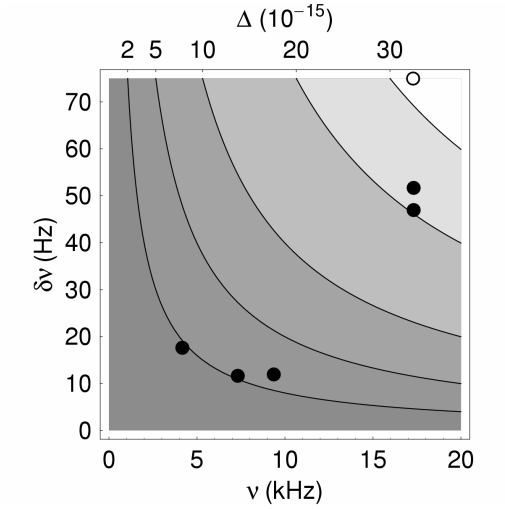

Figure 3. Uncertainty Δ in the second-order Zeeman correction (contours) as a function of Larmor frequency ν and its uncertainty δν obtained from the FWHM of the Zeeman component. The open point corresponds to the preliminary frequency measurement [3], and the closed points to subsequent optimizations of the homogeneity of the applied magnetic field inside the stainless steel UHV chamber (these proved unstable). Values of δν below 1 Hz have been obtained in the new non-magnetic UHV chamber

III. A NON-MAGNETIC UHV CHAMBER IN CrCu

A. *Design of the Chamber*

There are three primary requirements on materials for a non-magnetic UHV chamber: negligible magnetic susceptibility ($\mu-1$); sufficient hardness to permit the use of copper gasket seals, for convenience; and surface properties consistent with UHV, in particular minimal outgassing. A number of materials meet all of these requirements, including for example Ti or certain alloys of Al. We selected the novel alloy chromium copper (CrCu; 99.1% Cu, >0.6% Cr, <0.1% Fe), for two main reasons.

The first and most important is that when appropriately prepared, this material has very low outgassing rates for hydrogen after only a low-temperature bakeout [9]. A prebake at over 400 °C acts to age-harden the material and also precipitates excess Cr at the surface. On exposure to air after the prebake, a chromium oxide layer is formed which provides a barrier to both uptake of hydrogen into the bulk and outgassing of remaining interstitial hydrogen. Only a low-temperature bakeout to 100 °C is then needed to attain UHV. The outgassing rate from CrCu has been measured at the 10^{-12} Pa m/s (hydrogen equivalent) level [10], over an order of magnitude below that from stainless steel. It is important for the Yb^+ standard to exclude hydrogen from the background gas in the linear trap region as far as possible, because the formation of YbH by photoassociation represents an additional loss mechanism from the trap.

The second particular advantage of CrCu follows from the low bakeout temperature, which means that a wide variety of low-temperature brazes can be used and greatly increases available options for sealing windows and viewports to CrCu flanges.

The cube design was completed following extensive development work together with the manufacturer [11]. The trap is contained in a 6" CrCu cube machined from a single billet, with knife-edges machined into each face for a 6" ConFlat flange and into truncated faces at each corner for 1.33" ConFlat flanges to give optical access along the diagonals. Two large viewports are made by sealing a Corning 7056 borosilicate glass window to an OFHC Cu collar and brazing the resulting assembly into a 6" CrCu ConFlat flange. The window glass has good transmission in the near UV, which is necessary for efficient detection of fluorescence on the Yb^+ resonance transition at 369 nm. A high-quality window is used for the input of the laser cooling beams to the trap region; this window is of fused silica sealed to a Mo sleeve and brazed into a 2.75" CrCu flange. A Woods horn is used to dump the cooling beams is constructed from Corning 7056 glass in the same way as the 6" viewports. A full nipple made from OFHC Cu brazed to 6" CrCu ConFlat flanges at either end supports the cube and trap; the nipple runs through apertures in the magnetic shields, with the trap inside and the rest of the vacuum system outside. Pumps, gauges and feedthroughs made of stainless steel and other magnetic materials are therefore separated as far as is practical from the trap region.

The system is assembled using 'taper seal' Cu gaskets [12] for improved reliability of the ConFlat seal, giving greater seal area at lower compression and reducing any risk of damage to the CrCu knife edges.

B. *Measurements in the New Chamber*

The non-magnetic chamber was successfully commissioned over a year ago. Some initial difficulties with the reliability of braze seals meant that the system was first assembled with one of the two 6" viewports made from stainless steel. Even with this viewport in place, we have been able to demonstrate greatly improved homogeneity of the magnetic field which is also stable over time. In particular, the width δν of the field-sensitive $M_F = 0 \rightarrow \pm 1$ Zeeman component has been reduced below 1 Hz. It is apparent from Fig. 3 that this represents a reduction in δν by two orders of magnitude from the preliminary measurement [3], and consequently a reduction in the uncertainty Δ of the second-order Zeeman shift by the same factor. We therefore believe that all systematic uncertainties are at the level of one to two parts in 10^{15} or below, with a combined absolute frequency uncertainty projected to be 4 parts in 10^{15} or better.

Work is currently in progress to verify this level of performance with a measurement of the hyperfine transition frequency to this uncertainty, but is complicated by the requirement for high-precision time transfer to the SI second at a comparable level as noted above. We note here that new research projects in two-way satellite and GPS carrier phase time and frequency transfer are already under way at NMIA [13].

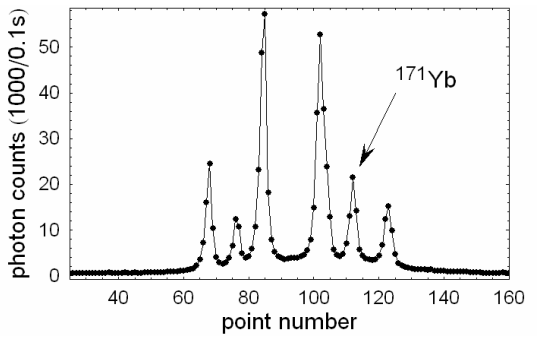

Figure 4. Fluorescence data on the 399 nm $^1S_1 \rightarrow {}^1P_1$ resonance transition of neutral Yb, obtained with a collimated oven. The laser frequency increases with point number across the sweep. An isolated hyperfine component of the ^{171}Yb isotope is shown [16]; this component allows loading of $^{171}Yb^+$ into the ion trap by isotope-selective photoionization [14].

The base pressure of the vacuum system is below 1×10^{-10} Torr, the same as the stainless steel system for the same pumping. However, the best test of background gas pressure and outgassing in the trap region itself is measurements of ion heating and trap loss rates, and these have not yet been completed.

IV. Photoionization

Loading the ion trap requires neutral Yb atoms produced from an effusive oven to be ionized in the trap region. Ionization is currently by electron impact, but photoionization [14] has two key advantages. First, it greatly reduces buildup of charge on insulated surfaces, and consequently also reduce stray DC and slowly-varying electric fields. Secondly, it allows selective loading of a single isotope from a Yb sample of natural isotopic abundance, which eliminates the need for isotope-enriched ^{171}Yb as used at present. Finally, greater loading efficiency at lower oven heating rates has been observed in other systems.

We have conducted a preliminary test of the use of photoionization to load Yb+ into the trap. The resonance transition of the neutral Yb atom ($^1S_0 \rightarrow {}^1P_1$) is at 399 nm; light at this wavelength was generated from the same Coherent Ti:sapphire laser normally used to generate 369 nm light for Yb^+, as we did not have an alternative source. Any wavelength shorter than 394 nm is then sufficient to excite from the $^1P_1$ state to above the ionization threshold. The second excitation stage was driven by light from a UV laser diode [15] operating near 369 nm (in principle, this near-UV light could also be generated by a UV LED). Because the diode laser was unfortunately not able to reach the Yb^+ 369 nm transition, it was necessary to retune the Ti:sapphire laser from 369 nm to 399 nm for loading and back to 369 nm to record Yb^+ fluorescence and characterize the load. This time-consuming process was nevertheless sufficient to confirm successful loading of the trap by photoionization.

Following this simple experiment the Yb oven was redesigned for greater collimation. Fig. 4 shows fluorescence recorded for the 399 nm transition of neutral Yb with the collimated oven. The observed hyperfine and isotopic structure is as expected [16], and it is apparent that one of the ^{171}Yb hyperfine components is sufficiently isolated to allow selective loading of this isotope.

V. Conclusion

The maximum achievable stability for a frequency standard based on laser-cooled $^{171}Yb^+$ ions is predicted to be better than $\sigma_y(\tau) = 5\times10^{-14}\ \tau^{-1/2}$, comparable to that already demonstrated at NMIA for buffer-gas cooled standards. This prediction assumes a cloud of radius 1 mm and length 10 mm containing approximately 10^4 ions, a Ramsey pulse separation of 10 s, and a cycle time of 13 s after allowing for cooling periods. Now that uncertainties associated with magnetic field inhomogeneity have been substantially reduced, we see no serious obstacle to realising a projected uncertainty of 4×10^{-15} or lower. Based on these estimates, a cloud of laser-cooled $^{171}Yb^+$ ions in a linear trap is projected to exhibit comparable performance to a cesium fountain, and continues to show significant promise as a frequency standard of both high accuracy and high stability.

Acknowledgments

The authors thank Dr A. G. Mann, Dr D. G. Blair and Dr M. E. Tobar of the Department of Physics, University of Western Australia, for the loan of the cryogenic sapphire resonator; Mr Colin Coles, for contributions to electronic and microwave engineering; Dr Stephen Lea of the National Physical Laboratory and Dr David Lucas of Oxford University, for correspondence regarding photoionization; and Mr Jed Bothell of Atlas UHV for development work on the non-magnetic UHV system.

References

[1] P. T. H. Fisk, M. J. Sellars, M. A. Lawn and C. Coles, "Accurate measurement of the 12.6 GHz 'clock' transition in trapped $^{171}Yb^+$ ions", IEEE Trans. Ultrasonics, Ferroelectrics and Frequency Control, vol. 44, pp. 344–354, 1997.

[2] P. T. H. Fisk, M. A. Lawn, and C. Coles, "Progress on the CSIRO trapped ytterbium ion clocks", in Proceedings of the Workshop on the Scientific Applications of Clocks in Space, NASA Jet Propulsion Laboratory Publication 97-15, 1997, pp. 143–152.

[3] R. B. Warrington, P. T. H. Fisk, M. J. Wouters and M. A. Lawn, "A microwave frequency standard based on laser-cooled $^{171}Yb^+$ ions", in Proceedings of the Sixth Symposium on Frequency Standards and Metrology, St Andrews 2001, World Scientific, 2002, pp. 297–304.

[4] R. B. Warrington, P. T. H. Fisk, M. J. Wouters, M. A. Lawn and C. Coles, "The CSIRO trapped $^{171}Yb^+$ ion clock: improved accuracy through laser-cooled operation", in Proceedings of the 1999 Joint Meeting EFTF and IEEE FCS, IEEE 99CH36313, 1999, pp. 125–128.

[5] R. B. Warrington, P. T. H. Fisk, M. J. Wouters and M. A. Lawn, "Temperature of laser-cooled $^{171}Yb^+$ ions and application to a microwave frequency standard", IEEE Trans. Ultrasonics, Ferroelectrics and Frequency Control, vol. 49, pp. 1166–1174, 2002.

[6] A. J. Giles, A. G. Mann, S. K. Jones, D. G. Blair and M. J. Buckingham, "A very high stability sapphire-loaded superconducting cavity oscillator", Physica B, vol. 165, pp. 145–6, 1990.

[7] L. Turner, Phys. Fluids, vol. 30, pp. 3196–3203, 1987.

[8] M. Drewsen, C. Brodersen, L. Hornekær, J. S. Hangst and J. P. Schiffer, "Large ion crystals in a linear Paul trap", Phys. Rev. Lett, vol. 81, pp. 2878–81, 1998.

[9] F. Watanabe, “Mechanism of ultralow outgassing rates in pure copper and chromium–copper alloy vacuum chambers: Reexamination by the pressure-rise method”, J. Vac. Sci. Tech. A, vol. 19, pp. 640–645, 2001.

[10] Y. Koyatsu, H. Miki and F. Watanabe, “Measurements of outgassing rate from copper and copper alloy chambers”, Vacuum, vol. 47, pp. 709–711, 1996.

[11] Atlas Technologies, www.atlasuhv.com.

[12] S. Kurokouchi, S. Morita and M. Okabe, “Characteristics of a taper-seal gasket for the Conflat sealing system”, J. Vac. Sci. Tech. A, vol. 19, pp. 2963–7, 2001.

[13] R. B. Warrington *et al*, ‘Time and Frequency Activities at the National Measurement Institute, Australia’, these proceedings; R. B. Warrington *et al*, ‘GPS Activities at the National Measurement Institute, Australia’, these proceedings.

[14] See for example N. Kjærgaard, L. Hornekær., A. M. Thommesen, Z. Videsen and M. Drewsen, “Isotope selective loading of an ion trap using resonance-enhanced two-photon ionization”, Appl. Phys. B, vol. 71, pp. 207–210, 2000.

[15] Nichia Corporation, www.nichia.co.jp.

[16] A.-M. Mårtensson Pendrill, D. S. Gough and P. Hannaford, “Isotope shifts and hyperfine structure in the 369.4-nm $6s$-$6p_{1/2}$ resonance line of singly ionized ytterbium”, Phys. Rev. A, vol. 49, pp. 3351–65, 1994.